applied nano

MDPI

Article

Catalase Like-Activity of Metal NPs–Enzyme Biohybrids

Noelia Losada-Garcia, Alba Rodriguez-Otero, Clara Ortega-Nieto, Ariane Azarmi and Jose M. Palomo *

Instituto de Catálisis y Petroleoquímica (ICP), CSIC, C/Marie Curie 2, 28049 Madrid, Spain
* Correspondence: josempalomo@icp.csic.es

Abstract: In this work, an efficient synthesis of bionanohybrids as artificial metalloenzymes (Cu, Pd, Ag, Mn) based on the application of an enzyme as a scaffold was described. Here we evaluated the effect of changing the metal, pH of the medium, and the amount of enzyme in the synthesis of these artificial metalloenzymes, where changes in the metal species and the size of the nanoparticles occur. These nanozymes were applied in the degradation of hydrogen peroxide for their evaluation as mimetics of catalase activity, the best being the **Mn@CALB-H_2O**, which presented MnO_2 nanostructures, with three-fold improved activity compared to Cu_2O species, **CuNPs@CALB-P**, and free catalase.

Keywords: metal bionanohybrids; nanozymes; catalase-like activity; hydrogen peroxide

check for updates

Citation: Losada-Garcia, N.; Rodriguez-Otero, A.; Ortega-Nieto, C.; Azarmi, A.; Palomo, J.M. Catalase Like-Activity of Metal NPs–Enzyme Biohybrids. *Appl. Nano* **2022**, *3*, 149–159. https://doi.org/10.3390/applnano3030011

Academic Editor: Angelo Maria Taglietti

Received: 16 June 2022
Accepted: 12 July 2022
Published: 7 August 2022

1. Introduction

Hydrogen peroxide (H_2O_2) is a by-product produced within the cells of living organisms and has detrimental effects on them [1–4]. Catalases are enzymes used by cells to remove excess cytoplasmic hydrogen peroxide by converting them to water and molecular oxygen. However, if the concentration of H_2O_2 increases due to disease, radiation exposure, and certain chemicals and medications that exceed the capacity of catalase, H_2O_2 begins to accumulate and cause cell damage [5–8]. On the other hand, the activity of the catalase enzyme can be affected by different environmental conditions, such as ionic strength, pH, and temperature (T), or due to the presence of compounds that inhibit its activity [9,10].

The rapid development of nanotechnology in recent decades has led to the creation of numerous catalytically active nanomaterials [11]. Currently, nanomaterials of different natures are widely used in biology, medicine, and biotechnology. This category includes nanomaterials with enzyme-mimetic properties, such as metallic and non-metallic nanoparticles, their oxides, magnetic nanoparticles, liposomes, and polymeric and carbon-based materials [12–14]. The ability of these nanomaterials to replace specific enzymes may offer new opportunities for enzyme-based applications such as immunoassays, biosensors, pharmaceutical processes, oncotherapy, the food industry, ecology, etc. [15–18]. This demonstrates the great importance of and commercial interest in the use of nanomaterials as enzyme mimetics. Compared with natural enzymes, nanozymes with inherent enzyme activities have recently attracted considerable attention due to their easy preparation, storage, and separation, as well as low cost [18,19].

One of the most used metals in the formation of artificial metalloenzymes is copper, due to its abundance, low cost, and low toxicity. Although most of the activities described in the literature are for Cu(II) materials, in fact, recently, in our group, Cu(II)-nanozymes with catalase activity were developed [20].

In this work, we describe the synthesis of highly stable heterogeneous metal (Cu, Mn, Pd, and Ag) nanoparticle catalysts (metal NPs–enzyme biohybrids), where the NPs were created in situ from an aqueous solution of the metal salt (Figure 1A) [21,22]. In addition, we have shown that these bionanohybrids of different natures, for example, other copper species and different metals, behaviors, and sizes, have the ability to completely mimic the particular enzymatic activity of catalase, even improving its activity (Figure 1B).

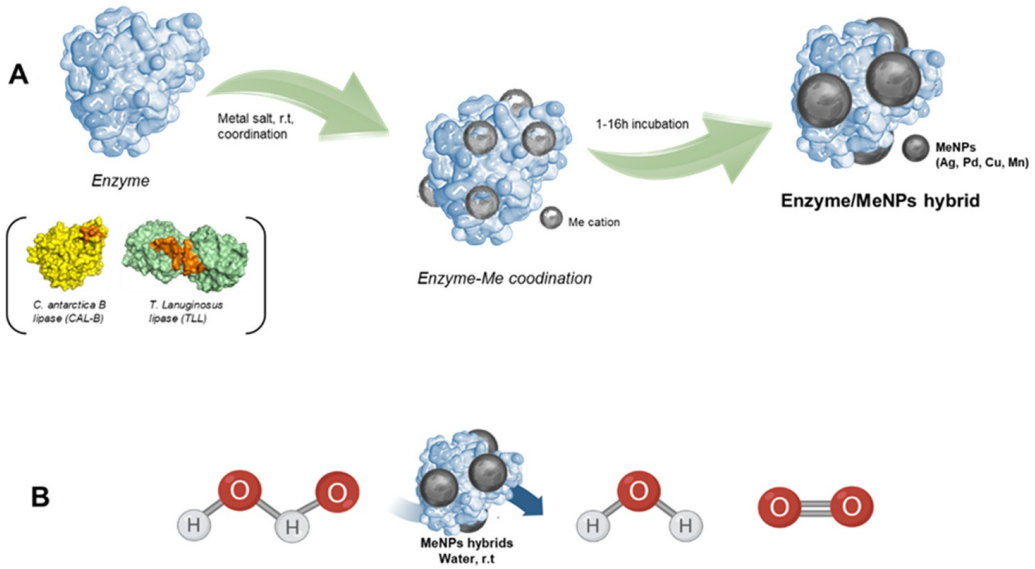

Figure 1. (**A**) Metal nanoparticle–enzyme hybrid synthesis; (**B**) catalase–like activity of different biohybrids. Me: metal, NP: nanoparticles.

2. Materials and Methods

2.1. Materials

Lipase B from *Candida antarctica* (CALB) solution and Catazyme® 25 L (catalase from *Aspergillus niger*) were purchased from Novozymes (Copenhagen, Denmark). Copper (II) sulfate pentahydrate [$Cu_2SO_4 \times 5H_2O$], N,N-dimethylformamide (DMF), and hydrogen peroxide (33% *v*/*v*) were from Panreac (Barcelona, Spain). Sodium bicarbonate, sodium phosphate, sodium borohydride, potassium permanganate, Tris base, and sodium tetrachloropalladate (II) were purchased from Sigma-Aldrich (St. Louis, MO, USA). Silver nitrate and MES were purchased from Thermo Fisher (Whaltam, MA, USA).

2.2. Characterization Techniques Used

Inductively coupled plasma–optical emission spectrometry (ICP–OES) was performed on an OPTIMA 2100 DV instrument (PerkinElmer, Waltham, MA, USA). X-ray diffraction (XRD) patterns were obtained using a Texture Analysis D8 Advance Diffractometer (Bruker, Billerica, MA, USA) with Cu Kα radiation. Transmission electron microscopy (TEM) and high-resolution TEM microscopy (HRTEM) images were obtained on a 2100F microscope (JEOL, Tokyo, Japan). Scanning electron microscopy (SEM) imaging was performed on a TM-1000 microscope (Hitachi, Tokyo, Japan). To recover the biohybrids, a Biocen 22 R (Orto-Alresa, Ajalvir, Spain) refrigerated centrifuge was used. Spectrophotometric analyses were run on a V-730 spectrophotometer (JASCO, Tokyo, Japan).

2.3. Synthesis of CuNPs@CALB Bionanohybrids

A total of 3.6 mL of commercial lipase B from *Candida antarctica* solution (CALB; 10 mg/mL) was added to 60 mL buffer 0.1 M (sodium phosphate pH 7.0) in a 250 mL glass bottle containing a small magnetic bar stirrer. Then, 600 mg of $Cu_2SO_4 \times 5H_2O$ (10 mg/mL) was added to the protein solution, and it was maintained for 16 h. After 16 h, 6 mL of $NaBH_4$ (300 mg) aqueous solution (1.2 M) was added to the cloudy solution (in two amounts of 3 mL). The solution turned rapidly black, and the mixture was reduced for 30 min. After the incubation, in all cases, the mixture was centrifuged at 8000 rpm for 5 min (10 mL per falcon-type tube of 15 mL). The generated pellet was re-suspended in 15 mL of distilled water. It was centrifuged again at 8000 rpm for 5 min at RT, and the supernatant removed. The process was repeated twice more. Finally, the supernatant was removed, and the pellet was re-suspended in 2 mL of distilled water, transferred to a cryotube, frozen with liquid nitrogen, and lyophilized overnight. After that, approximately 150 mg of black

solid was obtained. The hybrid was called **CuNPs@CALB-P**. Another variation of the protocol was avoiding the lyophilization step, conserving the catalyst as liquid suspension. This was called **CuNPs@CALB-P-NL**.

Other hybrids were synthesized following the previously established protocols under different conditions of pH, drying, and reduction (Table S1) which were tested in our work [23]. These bionanohybrids were called **CuNPs@CALB-P***, **CuNPs@CALB-B**, and **CuNPs@CALB-B***.

2.4. Synthesis of MnNPs@CALB Bionanohybrids

2.4.1. Method 1

A total of 3 mL of commercial CALB solution (10 mg/mL) was added to 100 mL sodium phosphate buffer 0.1 M pH 7.0 in a 250 mL glass bottle containing a small magnetic bar stirrer. Then, 70 mg of $MnSO_4 \times 5H_2O$ (0.7 mg/mL) was added to the protein solution and maintained for 16 h. After 16 h, 6 mL of $NaBH_4$ (300 mg) aqueous solution (1.2 M) was added to the cloudy solution (in two amounts of 3 mL) as a reducing agent. The mixture was reduced for 30 min. After the incubation, the mixture was centrifuged at 8000 rpm for 5 min at RT (10 mL per falcon type tube of 15 mL). The generated pellet was re-suspended in 15 mL of distilled water. It was centrifuged again at 8000 rpm for 5 min, and the supernatant was removed. The process was repeated twice more. Finally, the supernatant was removed, and the pellet of each falcon was re-suspended in 2 mL of distilled water; all solutions were collected in a round-bottom flask, frozen with liquid nitrogen, and lyophilized for 16 h. After that, 47 mg of the **MnNPs@CALB-P** was obtained.

Another variation of the protocol was the omission of the reduction step using sodium phosphate buffer 25 mM at pH 8.5. After that, 58 mg of the **MnNPs@CALB-P-NR** was obtained.

2.4.2. Method 2

$KMnO_4$ (500 mg) was dissolved in 10 mL of DMF or distilled water. This solution was added to 40 mL of a distilled water solution containing 2 mL of CALB (10 mg/mL). The final solution was kept under gentle magnetic stirring for 24 h at room temperature (RT). After that, the resulting suspension was separated by centrifugation (10,000 rpm; 4 °C; 15 min). The recovered pellet was washed once with 10 mL of distilled water containing 20% (*v*/*v*) of the corresponding co-solvent and twice with distilled water (2 × 10 mL). After this, the suspension was directly lyophilized to obtain the catalyst as a powder for later use. After that, approx. 350 mg of each bionanohybrid was obtained, called **MnNPs@CALB-H_2O** and **MnNPs@CALB-DMF**, respectively.

2.5. Synthesis of MeNPs@CATb Bionanohybrids

$AgNO_3$ (20 mg) or Na_2PdCl_4 (10 mg) were dissolved in 5 mL of distilled water solution containing 7.5 mg of bovine catalase (CATb). The solution was kept under gentle magnetic stirring for 24 h at RT. After that, the resulting suspension was separated by centrifugation (8000 rpm; 4 °C; 15 min). The recovered pellet was washed three times with 10 mL of distilled water. Afterwards, the suspension was directly lyophilized. The bionanohybrids were called **AgNPs@CATb** and **PdNPs@CATb**.

Characterization of the different metal bionanohybrids was performed by XRD, ICP–OES, TEM, HR-TEM, and SEM analysis.

2.6. Catalase-like Activity of Metal Bionanohybrids

Hydrogen peroxide (H_2O_2) (33% (*w*/*w*)) solution was prepared by adding 52 µL of hydrogen peroxide to 9.8 mL of 100 mM or 5 mM phosphate buffer (pH 6.0, pH 7.0, and pH 8.0), 5 mM tris base buffer pH 9, 5 mM MES buffer pH 5, or distilled water in order to obtaining a final concentration of 50 mM. The solution pH was adjusted using HCl or NaOH 1 M. To start the reaction, different amounts of MeNPs hybrids (2 mg or 4.5 mg) or 50 µL of Catazyme® 25 L (31 mg/mL) were added to 3 or 10 mL of the 50 mM solution

at RT. The reaction was followed by measuring the degradation of hydrogen peroxide recording the decrease of absorbance by spectrophotometry at 240 nm in quartz cuvettes of 1 cm path length by adding 2 mL of this solution at different times. Experiments were performed in triplicate.

In order to determine the catalase activity for each catalyst, the ΔAbs/min value was calculated using the linear portion of the curve (ΔAbs_s). The specific activity (U/mg) was calculated using the following equation:

$$U\left(\mu mol \cdot min^{-1} \cdot mg^{-1}\right) = \Delta Abs/min \cdot V \cdot \frac{1000}{\varepsilon \cdot mg_{catalyst}} \quad (1)$$

where the molar extinction coefficient (ε) used was 43.6 $M^{-1}cm^{-1}$, and $mg_{catalyst}$ refers to mg of enzyme or hybrid metal.

3. Results

3.1. Synthesis and Characterization of MeNPs@Enzyme Biohybrids

The synthesis of MeNPs@Enzyme biohybrids was performed in an aqueous medium by using a commercial solution of lipase B from *Candida antarctica* (CAL-B) or bovine catalase (CATb). This enzyme was previously dissolved in distilled water, and metal salt was previously dissolved in co-solvent (20% (*v*/*v*)) or added directly to the aqueous solution at RT and under gentle stirring. After 30 min, the initial clear solution turned to a slight cloudy suspension, which was completely cloudy after 16–24 h incubation. A solid was easily obtained after centrifugation, which was washed with the same reaction solvent first and distilled water after and finally frozen in liquid nitrogen and lyophilized, yielding the MeNPs@CALB hybrid. In some cases, it was necessary to add a reduction step using $NaBH_4$ after incubation, since although the CALB enzyme used as scaffold induces metal reduction, in metals with low reduction potential such as transition metals such as Cu, Fe, Mn, Zn, Co, etc., an additional reduction step is needed to achieve species from lower valence states.

Firstly, CuNPs@CALB biohybrids were analyzed by XRD, demonstrating differences in species, depending on the hybrids (Figure 2A). When the bionanohybrids presented 0.6 mg/mL of enzyme, **CuNPs@CALB-P** and **CuNPs@CALB-B** were obtained. In these catalysts, almost unique copper species, Cu_2O (matched well with JCPDS card no. 05-0667) or Cu(0) (matched well with JCPDS card no. 04-0836), respectively, could be seen. However, when the amount of enzyme was lower (0.3 mg/mL), hybrids synthesized by these protocols, **CuNPs@CALB-P*** and **CuNPs@CALB-B***, contained both copper species, Cu_2O and Cu(0). In the case of **CuNPs@CALB-P***, it presented 40% Cu(0) (Figure 2A), and in the case of **CuNPs@CALB-B*,** it presented 30% Cu(I) species. These differences could be due to the effect that the enzyme performs in the reduction step, since the protein environment slows down the reduction process. The TEM analysis demonstrated the formation of nanoparticles with a different diameter size (Figures 2 and S1), in a range between 6 and 15 nm (Table S1), the smallest ones being in **CuNPs@CALB-B** (Figure S1D).

Another modification of the synthesis protocol was the elimination of the lyophilization step, resulting in the production of **CuNPs@CALB-P-NL**. Analyzing the XRD pattern, the non-freezing of the enzyme structure could be observed; the species of this bionanohybrid presented a mixture of copper species [Cu_2O and Cu(0) (75:25 Cu_2O:Cu(0))]. TEM analysis demonstrated that the diameter size of the nanoparticles was the same as **CuNPs@CALB-P**, namely, 10 nm (Table S1).

The Cu amount on the solid was determined by ICP–OES analyses. The percentages of copper in the different CuNPs@CALB hybrids were 45% to 93% (Table S1).

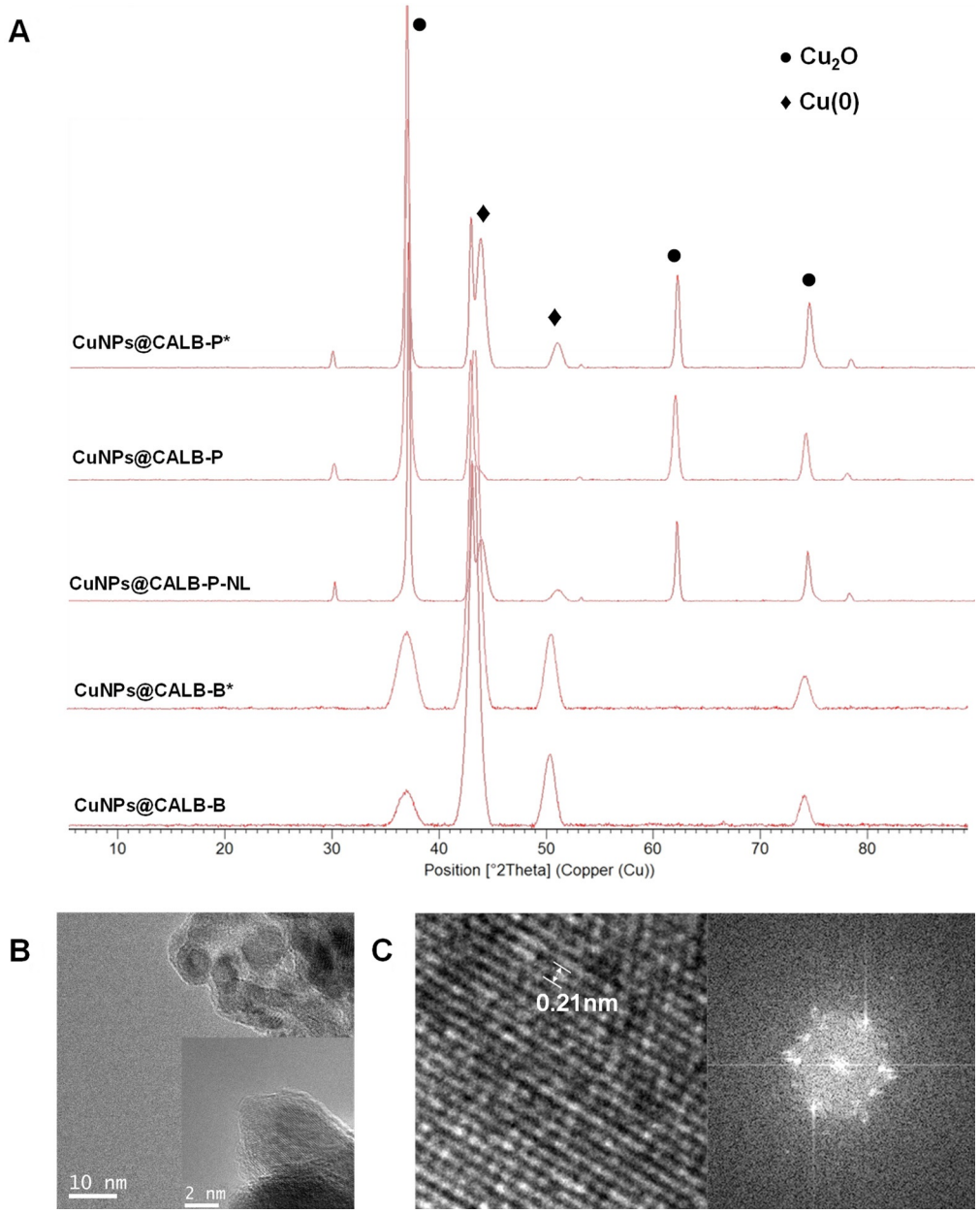

Figure 2. (**A**) XRD spectrum of CuNPs@CALB hybrids; (**B**) TEM and HR-TEM (inset) images of **CuNPs@CALB-P**; (**C**) FFT analysis of **CuNPs@CALB-P**.

Subsequently, a manganese salt ($MnSO_4$ salt) in sodium phosphate buffer was used. In this case, **MnNPs@CALB-P** or **MnNPs@CALB-P-NR** were obtained, respectively. The XRD pattern showed the same manganese species in both cases, namely, $Mn_3(PO_4)_2{\cdot}3H_2O$ (Figure 3A) [24]. SEM analysis showed similar mesoporous structures (Figure 3B,C). This shows that the reduction step did not have any consequence.

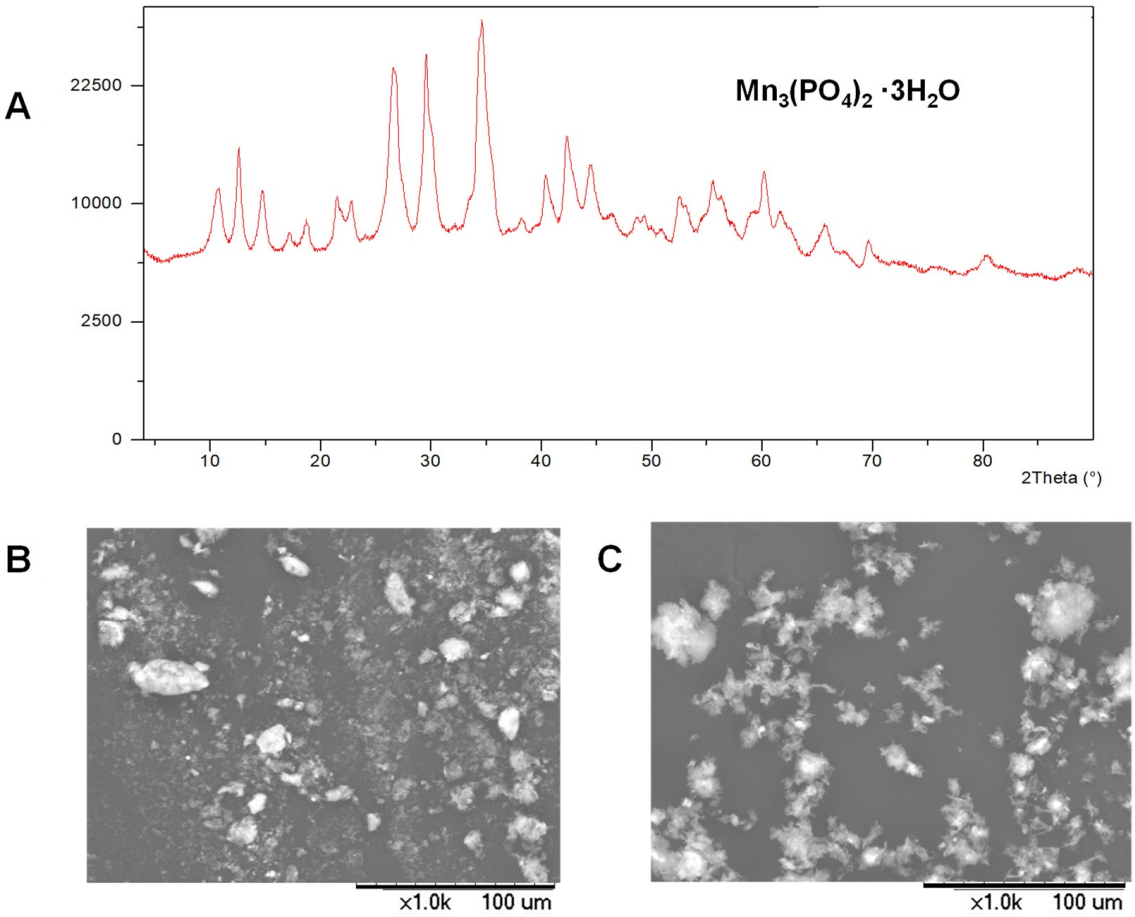

Figure 3. Characterization of MnNPs@CALB hybrids: (**A**) XRD spectrum; (**B**) SEM images of **MnNPs@CALB-P**; (**C**) SEM images of **MnNPs@CALB-P-NR**.

In addition, bionanohybrids were also prepared using $KMnO_4$ directly in distilled water or in the presence of DMF (20% v/v), obtaining **MnNPs@CALB-H_2O** and **MnNPs@CALB-DMF**, respectively. The XRD spectrum revealed the presence of MnO_2 (JCPDS card no 18-0802) in both catalysts (Figure 4A) [25]. SEM images showed amorphous chunks, and no crystallographic plains were observed in TEM analysis (Figure 4B,C).

The amount of Mn in the solid in each case was around 25%, determined by ICP–OES analysis (Table S1).

In addition to the metal change, another variation of the system was the introduction of other enzymes as scaffold, bovine catalase (CATb). As other metals, silver ($AgNO_3$) and palladium (Na_2PdCl_4) were used, to obtain **AgNPs@CATb** and **PdNPs@CATb**, respectively.

For the synthesis of the **AgNPs@CATb** hybrid, different Ag species were formed, namely, Ag(0), Ag_2O, and AgO, as observed in the XRD spectrum (Figure 5A(I)). SEM analysis demonstrated an aggregate with a mesoporous amorphous superstructure, and TEM images showed nanoparticles with a size between 10 and 20 nm due to the different species formed (Figures 5A(II,III) and S2). The amount of Ag was 34%, determined with ICP–OES analysis (Table S1).

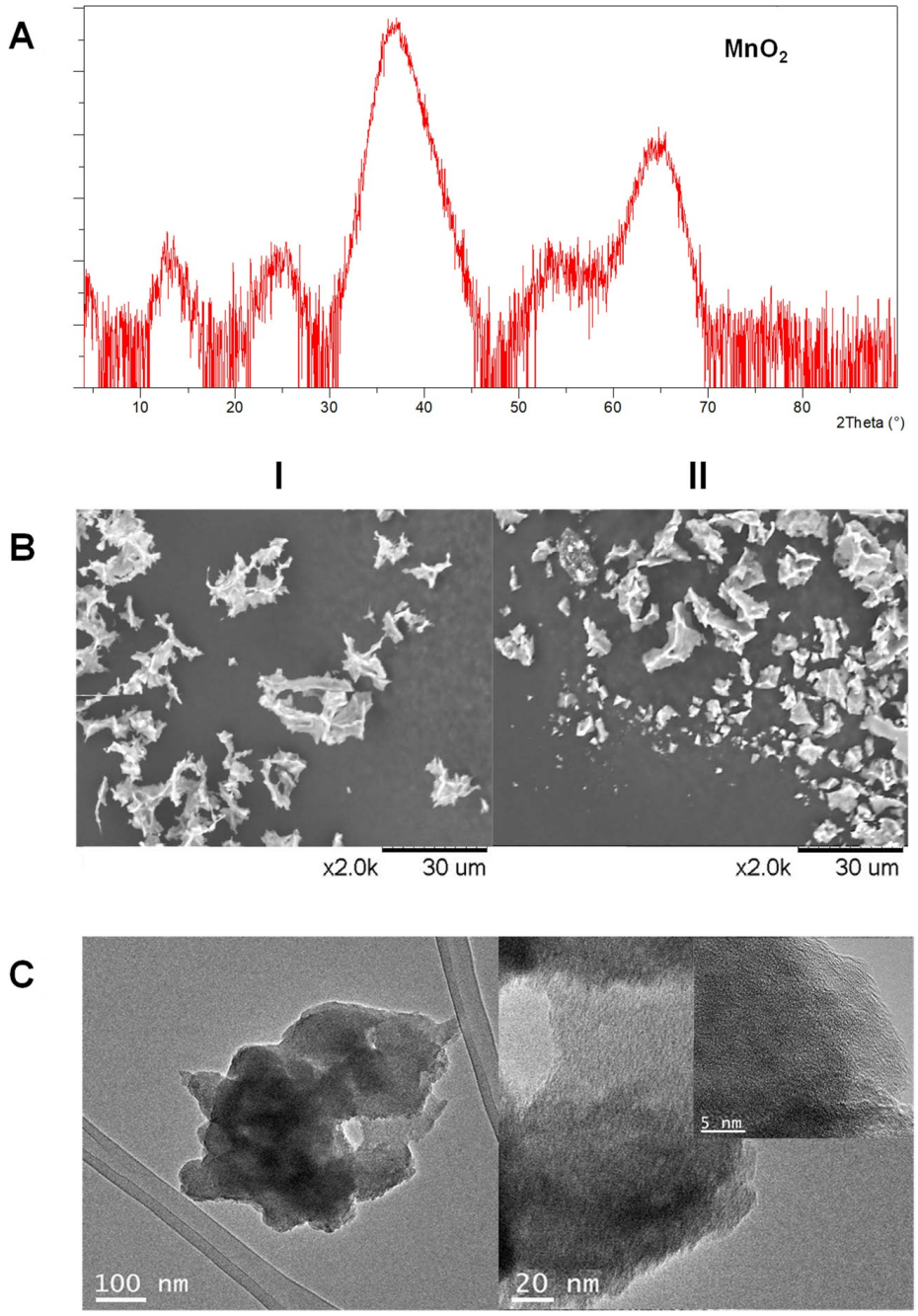

Figure 4. Characterization of **MnNPs@CALB-H_2O** and **MnNPs@CALB-DMF** hybrids: (**A**) XRD spectrum; (**B**) SEM images: (I). **MnNPs@CALB-H_2O** and (II). **MnNPs@CALB-DMF**; (**C**) TEM images of **MnNPs@CALB-DMF**.

On the other hand, **PdNPs@CATb** was synthesized with bovine catalase as the scaffold. The XRD spectrum evidenced the existence of palladium chloride nanoparticles (Figure 5B(I)) [26]. SEM analysis demonstrated mesoporous structures, and TEM images showed the formation of small spherical nanoparticles with an average diameter of 10 nm (Figures 5B(II,III) and S3). The amount of Pd was 27%, as determined by ICP–OES analysis (Table S1).

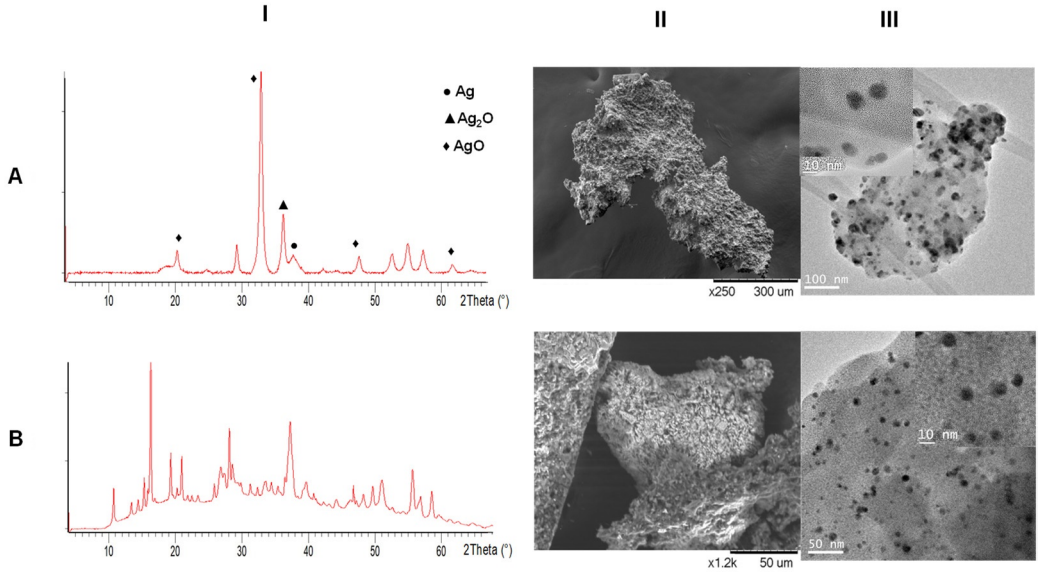

Figure 5. (**A**) **AgNPs@CATb** hybrid characterization; (**B**) **PdNPs@CATb** hybrid characterization. (I) XRD spectrum; (II) SEM images; (III) TEM images and HR-TEM (inset).

3.2. Catalase-like Activity of Different MeNPs Biohybrids

Firstly, the Cu hybrids were evaluated for H_2O_2 degradation in distilled water (Figure 6A). In general, all the copper catalysts demonstrated catalase activity, where **CuNPs@CALB-P** was the most efficient biocatalyst with specific activity of 2.5 U/mg. This was due to the presence of a unique species of copper, namely, Cu_2O. Comparing this result with the rest of the copper catalysts, **CuNPs@CALB-P*** showed 5.5 times less activity. In the case of the catalyst synthesized at pH 10.0, it can be observed that the activity of **CuNPs@CALB-B***, which had a greater presence of oxidized species, was only two times lower, while **CuNPs@CALB-B**, which had mostly Cu(0), presented half the activity of **CuNPs@CALB-B***. The obtained results clearly demonstrated that the decomposition of hydrogen peroxide was more efficient for Cu(I) species.

On the other hand, other tests were carried out in buffer solutions with low or high ionic strength (5 mM and 100 mM) in a pH range of 6.0 to 8.0 (Figure 6B,C). In these cases, a general decrease in the activity of all catalysts was observed, even at very low buffer amounts. Specifically, at a low ionic strength, when the pH was higher, they presented higher catalase activity, although in the case of **CuNPs@CALB-P**, at any pH, it presented activity at least six times lower than in distilled water. When the medium had a high ionic strength, the results were worse for all cases.

These effect of inhibition of phosphate ions in the degradation of hydrogen peroxide by the copper nanoparticles could be explained considering some kind of binding of a phosphate group to the copper, generating intermediate species and reducing the reactivity of the catalyst. Indeed, this can be supported by the results obtained when a hybrid containing copper phosphate species [23] was used. In this case the catalase activity of this hybrid was more than 20 times lower in distilled water than the Cu hybrids present in this work (data not shown).

Therefore, for the conditions of greatest activity in **CuNPs@CALB-P** (distilled water), the catalase activity of the same hybrid was evaluated but without lyophilization treatment (Figure 6D) (**CuNPs@CALB-P-NL**), where a 5.5-fold lower activity was observed, demonstrating the effect of the presence of Cu(0) species. Finally, the activity of **CuNPs@CALB-P** was compared with the activity of free catalase (Figure 6D), where an activity of 90% could be observed.

After that, we evaluated the MnNPs@CALB hybrids under the best conditions previously studied for copper, that is, in distilled water (Figure 7). Catalysts **MnNPs@CALB-P** and **MnNPs@CALB-P-NR**, which have a manganese phosphate species, had no activity.

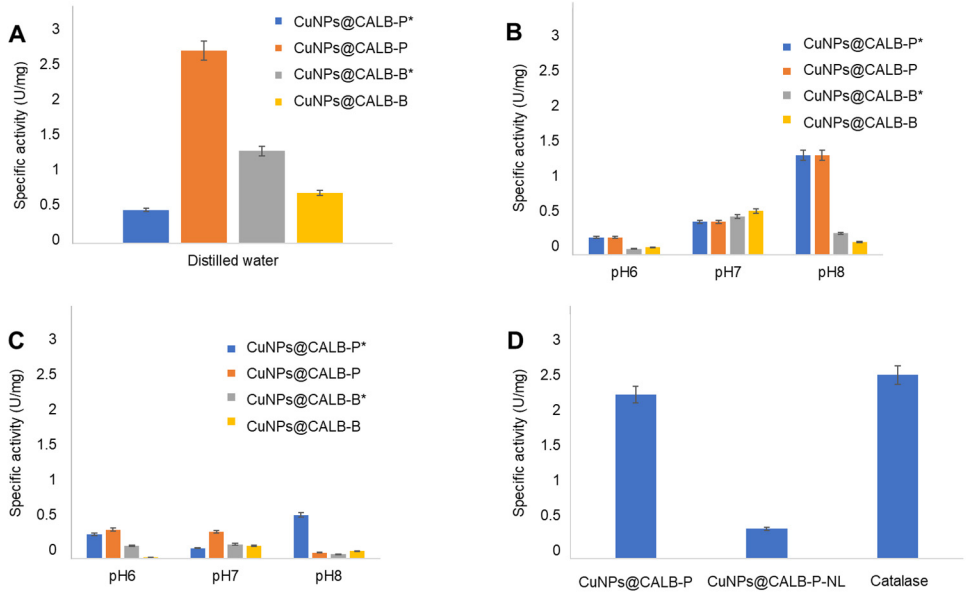

Figure 6. Catalase-like activity of different CuNPs@CALB hybrids. (**A**) Distilled water; (**B**) sodium phosphate buffer 5 mM; (**C**) sodium phosphate buffer 100 mM; (**D**) **CuNPs@CALB-P** in distilled water compared with free catalase and **CuNPs@CALB-P-NL**.

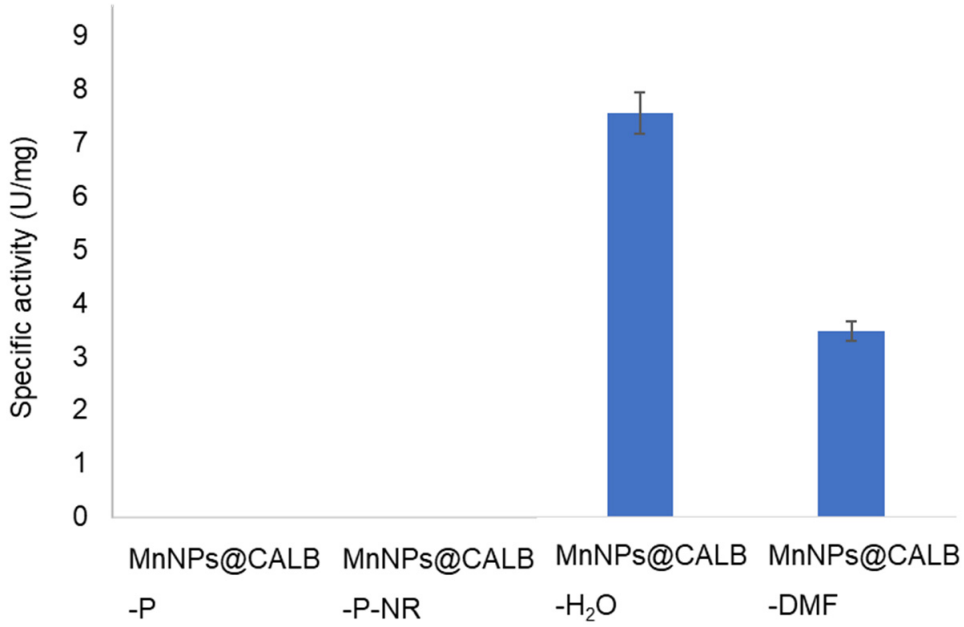

Figure 7. Catalase-like activity of MnNPs@CALB hybrids in distilled water.

On the other hand, when the species were MnO_2 nanostructures, **MnNPs@CALB-H_2O** presented the highest activity, being 2.2 times higher than **MnNPs@CALB-DMF**. Furthermore, these catalysts were evaluated in other reaction media such as 5 mM tris base buffer pH 9 and 5 mM MES buffer pH 5 (Figure S4). In these cases, the negative effect generated by the presence of ionic strength could be observed, as in the case of copper mentioned above, where the activity in both catalysts at a pH similar to that of distilled water, such as that of the MES buffer, was 45-fold lower for **MnNPs@CALB-H_2O** and 4.5-fold lower for **MnNPs@CALB-DMF**. In the case of a buffer with a higher pH (pH 9), for **MnNPs@CALB-DMF** it presented similar activity, while for **MnNPs@CALB-H_2O** it was half (Figure S4).

Finally, the **MnNPs@CALB-H_2O** biohybrid exhibited activity three times higher than that of natural catalase at RT in distilled water (Figure 7).

Finally, two biohybrids of precious metals (Ag and Pd) were synthesized using bovine catalase as a scaffold (**AgNPs@CATb** and **PdNPs@CATb**) to evaluate a potential synergistic effect between catalase and metal nanoparticles. However, the specific activity of both catalysts was very low (more than 100 times lower than the Mn hybrid) (data not shown). These could be due to the type of metal species formed in each case, namely, $PdCl_2$ for the Pd hybrid, and a mixture of different silver oxides for the Ag hybrid.

In the literature, there are different methodologies for the degradation of H_2O_2 as a mimetic of catalase activity. Some of them use complexes of precious metals, in some cases supported, or tubular structures, where it is necessary to synthesize systems under drastic and toxic conditions [27–30]. Therefore, the methodology proposed in our work has an advantage regarding simplicity and sustainability in the creation of artificial metalloenzymes capable of degrading H_2O_2 in aqueous medium at RT.

4. Conclusions

In conclusion, in this study we have presented a simple but versatile strategy for preparation of different catalase-like activity artificial metalloenzymes (MeNPs@Enzyme) based on the application of an enzyme that induces the in situ formation of metal nanoparticles on the protein network.

Different bionanohybrids of different metals (Cu, Mn, Pd, Ag) were synthesized and evaluated in terms of their ability to decompose hydrogen peroxide at RT in aqueous media. **MnNPs@CALB-H_2O**, formed by MnO_2 nanostructures, presented excellent mimetic activity, being even three times higher than natural catalase.

Therefore, these results open the potential application of these novel bionanohybrids in combination with other enzymatic systems for biological and biomedical processes.

Supplementary Materials: The following supporting information can be downloaded at: https://www.mdpi.com/article/10.3390/applnano3030011/s1, Figure S1. (I) TEM images; (II) HR-TEM images. (A) CuNPs@CALB-P*; (B) CuNPs@CALB-P-NL; (C) CuNPs@CALB-B*; (D) CuNPs@CALB-B. Figure S2. Characterization of AgNPs@CATb: (A) SEM images; (B) TEM image; Figure S3. Characterization of PdNPs@CATb: (A) SEM images; (B) TEM image; Figure S4. Catalase-like activity of MnNPs@CALB hybrids in 5 mM of TRIS BASE pH 9 (Blue) and 5 mM of MES pH 5 (Orange). Table S1. Synthesis of MeNPs@Enzyme hybrids.

Author Contributions: N.L.-G., A.R.-O., C.O.-N. and A.A. performed the experiments; J.M.P. designed and supervised the study and experiments; and J.M.P. and N.L.-G. wrote the manuscript. All authors have read and agreed to the published version of the manuscript.

Funding: This work was supported by the Spanish Government: the Spanish National Research Council (CSIC) (PTI-Health CSIC SGL2103036).

Data Availability Statement: Not applicable.

Acknowledgments: The authors thank Ramiro Martinez from Novozymes.

Conflicts of Interest: The authors declare no conflict of interest.

References

1. Wu, Z.; Liu, M.; Liu, Z.; Tian, Y. Real-time imaging and simultaneous quantification of mitochondrial H_2O_2 and ATP in neurons with a single two-photon fluorescence-lifetime-based probe. *J. Am. Chem. Soc.* **2020**, *142*, 7532–7541. [CrossRef] [PubMed]
2. Song, X.; Bai, S.; He, N.; Wang, R.; Xing, Y.; Lv, C.; Yu, F. Real-time evaluation of hydrogen peroxide injuries in pulmonary fibrosis mice models with a mitochondria-targeted near-infrared fluorescent probe. *ACS Sen.* **2021**, *6*, 1228–1239. [CrossRef] [PubMed]
3. Filip, C.; Albu, E. (Eds.) *Reactive Oxygen Species (ROS) in Living Cells*; IntechOpen: London, UK, 2018.
4. Bai, Z.; Li, G.; Liang, J.; Su, J.; Zhang, Y.; Chen, H.; Huang, Y.; Sui, W.; Zhao, Y. Non-enzymatic electrochemical biosensor based on PtNPs/RGO-CS-Fc nano-hybrids for the detection of hydrogen peroxide in living cells. *Biosens. Bioelectron.* **2016**, *82*, 185–194. [CrossRef] [PubMed]
5. Rasheed, R.T.; Mansoor, H.S.; Abdullah, T.A.; Juzsakova, T.; Al-Jammal, N.; Salman, A.D.; Al-Shaikhly, R.R.; Le, P.C.; Domokos, E.; Abdulla, T.A. Synthesis, characterization of V_2O_5 nanoparticles and determination of catalase mimetic activity by new colorimetric method. *J. Therm. Anal. Calorim.* **2021**, *145*, 297–307. [CrossRef]

6. Nandi, A.; Yan, L.J.; Jana, C.K.; Das, N. Role of catalase in oxidative stress- and age-associated degenerative diseases. *Oxid. Med. Cell. Longev.* **2019**, *13*, 123–132. [CrossRef]
7. Ali, F.; Manzoor, U.; Khan, F.I.; Lai, D.; Khan, M.K.A.; Chandrashekharaiah, K.S.; Singh, L.R.; Dar, T.A. Effect of polyol osmolytes on the structure-function integrity and aggregation propensity of catalase: A comprehensive study based on spectroscopic and molecular dynamic simulation measurements. *Int. J. Biol. Macromol.* **2022**, *209*, 198–210. [CrossRef]
8. Nantapong, N.; Murata, R.; Trakulnaleamsai, S.; Kataoka, N.; Yakushi, T.; Matsushita, K. The effect of reactive oxygen species (ROS) and ROS-scavenging enzymes, superoxide dismutase and catalase, on the thermotolerant ability of *Corynebacterium glutamicum*. *Appl. Microbiol. Biotechnol.* **2019**, *103*, 5355–5366. [CrossRef]
9. Fernandez-Lafuente, R. Stabilization of multimeric enzymes: Strategies to prevent subunit dissociation. *Enzyme Microb. Technol.* **2009**, *45*, 405–418. [CrossRef]
10. Hromic-Jahjefendic, A. Testing temperature and pH stability of the catalase enzyme in the presence of inhibitors. *Period. Eng. Nat. Sci.* **2022**, *10*, 18–29. [CrossRef]
11. Cormode, D.P.; Gao, L.; Koo, H. Emerging biomedical applications of enzyme-like catalytic nanomaterials. *Trends Biotechnol.* **2018**, *36*, 15–29. [CrossRef]
12. Jiao, M.; Li, Z.; Li, X.; Zhang, Z.; Yuan, Q.; Vriesekoop, F.; Liang, H.; Liu, J. Solving the H_2O_2 by-product problem using a catalase-mimicking nanozyme cascade to enhance glycolic acid oxidase. *Chem. Eng. J.* **2020**, *388*, 124249. [CrossRef]
13. Zhang, H.; Yang, K.L. In situ formation and immobilization of gold nanoparticles on polydimethylsiloxane (PDMS) exhibiting catalase-mimetic activity. *Chem. Commun.* **2020**, *56*, 6416–6419. [CrossRef]
14. Zhang, J.; Lu, X.; Tang, D.; Wu, S.; Hou, X.; Liu, J.; Wu, P. Phosphorescent carbon dots for highly efficient oxygen photosensitization and as photo-oxidative nanozymes. *ACS Appl. Mater. Interfaces* **2018**, *10*, 40808–40814. [CrossRef] [PubMed]
15. Chen, H.; Seiber, J.N.; Hotze, M. ACS select on nanotechnology in food and agriculture: A perspective on implications and applications. *J. Agric. Food Chem.* **2014**, *62*, 1209–1212. [CrossRef] [PubMed]
16. Chen, W.; Chen, J.; Feng, Y.B.; Hong, L.; Chen, Q.Y.; Wu, L.F.; Lin, X.-H.; Xia, X.-H. Peroxidase-like activity of water-soluble cupric oxide nanoparticles and its analytical application for detection of hydrogen peroxide and glucose. *Analyst* **2012**, *137*, 1706–1712. [CrossRef] [PubMed]
17. Lu, L.; Wang, X.; Xiong, C.; Yao, L. Recent advances in biological detection with magnetic nanoparticles as a useful tool. *Sci. China Chem.* **2015**, *58*, 793–809. [CrossRef]
18. Wang, Q.; Wei, H.; Zhang, Z.; Wang, E.; Dong, S. Nanozyme: An emerging alternative to natural enzyme for biosensing and immunoassay. *Trends Analyt. Chem.* **2018**, *105*, 218–224.
19. Wu, J.J.; Wang, X.Y.; Wang, Q.; Lou, Z.P.; Li, S.R.; Zhu, Y.Y.; Qin, L.; Wei, H. Nanomaterials with enzyme-like characteristics (nanozymes): Next-generation artificial enzymes (II). *Chem. Soc. Rev.* **2019**, *48*, 1004–1076. [CrossRef]
20. Losada-Garcia, N.; Jimenez-Alesanco, A.; Velazquez-Campoy, A.; Abian, O.; Palomo, J.M. Enzyme/nanocopper hybrid nanozymes: Modulating enzyme-like activity by the protein structure for biosensing and tumor catalytic therapy. *ACS Appl. Mater. Interfaces* **2021**, *13*, 5111–5124. [CrossRef]
21. Palomo, J.M. Nanobiohybrids: A new concept for metal nanoparticles synthesis. *Chem. Commun.* **2019**, *55*, 9583–9589. [CrossRef]
22. Filice, M.; Losada-Garcia, N.; Perez-Rizquez, C.; Marciello, M.; Morales, M.D.P.; Palomo, J.M. Palladium-nanoparticles BioHybrids in applied chemistry. *Appl. Nano* **2020**, *2*, 1–13. [CrossRef]
23. Losada-Garcia, N.; Rodriguez-Otero, A.; Palomo, J.M. Tailorable synthesis of heterogeneous enzyme–copper nanobiohybrids and their application in the selective oxidation of benzene to phenol. *Catal. Sci. Technol.* **2020**, *10*, 196–206. [CrossRef]
24. Munyemana, J.C.; He, H.; Ding, S.; Yin, J.; Xi, P.; Xiao, J. Synthesis of manganese phosphate hybrid nanoflowers by collagen-templated biomineralization. *RSC Adv.* **2018**, *8*, 2708–2713. [CrossRef] [PubMed]
25. Li, Y.; Xiao, L.; Liu, F.; Dou, Y.; Liu, S.; Fan, Y.; Cheng, G.; Song, W.; Zhou, J. Core-shell structure Ag@Pd nanoparticles supported on layered MnO_2 substrate as toluene oxidation catalyst. *J. Nanopart. Res.* **2019**, *21*, 28. [CrossRef]
26. Manepalli, R.K.N.R.; Madhav, B.T.P.; Giridhar, G.; Srinivasulu, M.; Tejaswi, M.; Sivaram, K.; Jayaprada, P.; Pisipati, V.G.K.M. Characterisation and mesomorphic behaviour of liquid crystals with dispersed $PdCl_2$ nanoparticles. *Liq. Cryst. Today* **2017**, *26*, 32–38. [CrossRef]
27. Chaibakhsh, N.; Moradi-Shoeili, Z. Enzyme mimetic activities of spinel substituted nanoferrites (MFe_2O_4): A review of synthesis, mechanism and potential applications. *Mater. Sci. Eng. C* **2019**, *99*, 1424–1447. [CrossRef]
28. Marr, K.M.; Chen, B.; Mootz, E.J.; Geder, J.; Pruessner, M.; Melde, B.J.; Vanfleet, R.R.; Mendintz, I.L.; Iverson, B.D.; Claussen, J.C. High aspect ratio carbon nanotube membranes decorated with Pt nanoparticle urchins for micro underwater vehicle propulsion via H_2O_2 decomposition. *ACS Nano* **2015**, *9*, 7791–7803. [CrossRef]
29. Zhang, H.; Deng, X.; Jiao, C.; Lu, L.; Zhang, S. Preparation and catalytic activities for H_2O_2 decomposition of Rh/Au bimetallic nanoparticles. *Mater. Res. Bull.* **2016**, *79*, 29–35. [CrossRef]
30. Yesmurzayeva, N.N.; Nurakhmetova, Z.A.; Tatykhanova, G.S.; Selenova, B.S.; Kudaibergenov, S.E. Catalytic activity of gold and silver nanoparticles supported on zinc oxide. *Supramol. Catal.* **2015**, *2*, 1–8. [CrossRef]